Desalination and Water Treatment
www.deswater.com

doi: 10.5004/dwt.2019.23920

147 (2019) 164–172
April

An investigation of dual-step ozone induced flotation (DOIF) process for tertiary wastewater treatment: characteristics of aerated flocs, removal performance and mechanism

Meiyan Liu[a], Lihui Zhou[b], Ning Liu[b], Xin Jin[a], Pengkang Jin[a,*], Xiaochang C. Wang[a]

[a]*Key Laboratory of Environmental Engineering, School of Environmental and Municipal Engineering, Xi'an University of Architecture and Technology, Xi'an, Shaanxi Province, 710055 Shaanxi, China, Tel. +86 13379217572; email: pkjin@hotmail.com (P. Jin), Tel. +86 18391481826; email: 2260255425@qq.com (M. Liu), Tel. +86 15991688026; email: jinxinjason2006@163.com (X. Jin), Tel. +86 13991976150; email: xcwang@xauat.edu.cn (X.C. Wang)*
[b]*Technology Research Institute, PetroChina Changqing Oilfield Company, Xi'an, Shaanxi Province 710018, China, Tel. +86 13572089939; email: zlh_cq@petrochina.com.cn (L. Zhou), Tel. +86 18502916086; email: liun15_cq@petrochina.com.cn (N. Liu)*

Received 24 February 2018; Accepted 23 January 2019

ABSTRACT

A novel dual-step ozone induced flotation (DOIF) process was developed for the application in wastewater reclamation, where ozonation, coagulation and separation occurred simultaneously. Compared with the dissolved-ozone flotation (DOF) process, an ozonation zone was added to further oxidize refractory contaminants by residual ozone gas. In this study, a pilot-scale DOIF system fed by secondary effluent from a municipal wastewater treatment plant in Xi'an, China, was used to evaluate its performance in tertiary wastewater treatment. The effect of main operating parameters (saturator pressure: 0.3, 0.4, 0.5 MPa; recycle ratio: 30%, 40% and 50%) involved were studied. The results showed that the favorable bubbles and aerated flocs were generated at 0.4 MPa and 30% recycle ratio. At the optimal operational condition, the DOIF process exhibited good performance of color, turbidity, UV_{254}, TP removal and disinfection in general. Moreover, extra ozonation can further improve the color, UV_{254} removal and disinfection performance. To interpret the mechanism of the DOIF process, para-chlorobenzoic acid (*p*CBA) removal, a hydroxyl radical (•OH) probe compound, was monitored. It was observed that the DOIF process generated more •OH in the presence of polyaluminium chloride. This indicates that the •OH oxidation reaction was involved in DOIF process to enhance the dissolved organic matter removal. The application of DOIF system in tertiary wastewater treatment can reduce the waste of ozone and improve the treatment efficiency.

Keywords: Dual-step ozone induced flotation (DOIF); Ozonation; Aerated flocs; Hydroxyl radical

1. Introduction

Dissolved air flotation (DAF) has been widely applied in water and wastewater treatment and reuse [1–3]. In addition, residual organic compounds in effluent wastewater have been identified as a major source of micropollutants, for instance, complex mixtures of natural organic matter from drinking water, soluble microbial products originating from the activated sludge (related to the sludge metabolism or decay) and refractory organics from industrial and residential origin [4]. Although the DAF process had a certain removal of COD, BOD_5 and TSS, the removal of dissolved organic matter needs further improvement [5–7].

Because of the powerful oxidation, ozone has been widely used in water and wastewater treatment as a disinfectant and oxidant [8–10]. Usually, ozone is used for various purposes

* Corresponding author.

such as removal of color [11,12] and natural refractory organic compounds [13]. Therefore, ozone can be applied as a substitute for air in the DAF system, thereby becoming dissolved-ozone flotation (DOF), an innovative wastewater reclamation process, which combines ozonation and flotation together.

Compared with the conventional tertiary wastewater treatment process, which comprises coagulation, sedimentation and filtration, the DOF process is superior in decolorization, odor and organic matter removal. Also, the hydraulic retention time of the DOF process is three times shorter than the conventional tertiary wastewater treatment process, which results in much less space requirements [14]. This is because coagulation, separation, decolorization, odor removal and disinfection could occur simultaneously in a DOF reactor [5,6,14]. At the same time, the previous study by Jin et al. [15] proposed a hybrid ozonation–coagulation process in which Al-based coagulants and hydrolyzed products could act as catalysts to enhance ozone decomposition into •OH when ozonation and coagulation occurred simultaneously within a single unit, thereby improving the organics removal efficiency. Thus, metal coagulants may function as the catalyst to facilitate •OH generation in the DOF process and to improve dissolved organic matter removal efficiency. Moreover, the ozonation–coagulation process still remained in laboratory study [15] and has never been investigated in pilot-scale unit or a full-scale plant. Although Zhang et al. [16] conducted a pilot study on removal efficiency of indicator compounds representative of pharmaceuticals and personal care products, coagulation and ozonation do not occur at the same time in a single reactor.

The previous study by Lee et al. [17] reported that ozone enhanced the separation capability of the DAF system not only by assisting the coagulation of dissolved contaminants but also by increasing the microbubble volume of the DOF system because ozone has a higher solubility in water than air. However, although application of ozone facilitates the conventional flotation removal efficiency, the solubility of ozone in the water is still limited. The solubility of ozone in water at 20°C, 0.45 MPa is 10% at pH 6.9–7.4. This means there was always a waste of ozone from the ozone generator. Therefore, on the basis of the DOF process, an ozonation zone was added to further oxidize refractory contaminants by residual ozone gas. Therefore, a dual-step ozone induced flotation (DOIF) process was first put forward to reduce the waste of ozone and further improve the treatment efficiency.

In this study, a pilot-scale DOIF system fed by secondary effluent from a wastewater treatment plant (WWTP) in Xi'an, China, was used to evaluate the tertiary wastewater treatment efficiency. First, to investigate the optimal operational condition in DOIF process, the effect of saturator pressure and recycle ratio on the bubbles and aerated flocs size distribution was investigated. Second, removal performance of color, turbidity, UV_{254}, TP and disinfection effect was investigated in DOIF process at optimal operational condition. Finally, in order to interpret removal performance of DOIF, the mechanism of DOIF process was revealed as well.

2. Materials and methods

2.1. Raw water

The water used in this study was effluent wastewater with pH of 6.9–7.4 collected before the disinfection step at the effluent of the sedimentation tank in a municipal WWTP in Xi'an, China. The WWTP consists of a biological anaerobic-anoxic-oxic (AAO) treatment process that mainly treats domestic wastewater. The capacity of the WWTP is 500,000 m^3 d^{-1} with hydraulic retention time of 20 h and sludge retention time of 19 d. The effluent of the WWTP typically has the following characteristics: color 2.6–3.1 c.u., turbidity 2.0–5.0 NTU, UV_{254} 0.12–0.13 cm^{-1}, TOC 5.0~8.0 mg L^{-1}, total phosphorus 0.1–0.3 mg L^{-1} and *Escherichia coli* 300–600 cfu mL^{-1}.

2.2. Experimental setup

The experimental setup of DOIF system is shown in Fig. 1. The major part of the DOIF separator is a closed cylindrical compartment with an inner column at the centre and a baffle, thus, dividing the cylindrical space into a contact zone, a separation zone and an ozonation reactor. On top of the compartment, there is an inversely placed circular cone forming a scum chamber. There are two inlets at the bottom of the separator. One serves as the entrance for the raw water, that is, the secondary effluent, after coagulant (polyaluminium chloride, PAC) dosing and mixing through the raw water pump and online hydraulic mixer. Another serves as the entrance for the return flow mixed with dissolved ozone. Next to the ozone dissolving pump and following the saturator, gaseous ozone from an ozone generator is dissolved in the water (return flow from the treated water) as micro bubbles. The two flows are well mixed under hydraulic conditions as they enter the contact zone from its bottom. Therefore, a contact reaction of ozone with pollutants and attachment of pollutants onto micro ozone bubbles occurs at the same time in the contact zone. In the separation zone, floated scum accumulates on the top and treated water is collected through the perforated annular pipe at the bottom and flow into ozonation reactor beneath the baffle. In the ozonation reactor, the effluent from the separation zone was further oxidized by using ozone which was not dissolved in the ozone dissolving pump. A magnetic valve is installed on the "inverted U-shaped tube", which is automatically controlled by a time controller so that it can be switched "open" and "closed" at pre-set time intervals. As the valve opens, treated water flows out of the DOIF separator at a regular rate and the water level decreases in the separator. As the valve closes, the treated water flow is shut down, and the water level begins to rise in the DOIF separator. In this way, scum accumulated on the top can get discharged. In addition, standard operational condition for the DOIF reactor is shown in Table 1.

2.3. Analytical methods

2.3.1. Aerated flocs characterization

Aerated flocs characterization technique was used to characterize multiphase system in flocculation–flotation processes, which takes into account the principle of atmospheric pressure balance. The main component of the aerated flocs characterization technique is the rising tube that consists of an acrylic circular tube with a total length of 45 cm and an inner diameter of 5 cm. Over the tube, there is a top rectangular acrylic box (10 cm × 10 cm × 15 cm) that has four glass windows on the lateral walls (15 cm × 7 cm each) and one on top (7 cm × 7 cm). Also, this box has an opening system

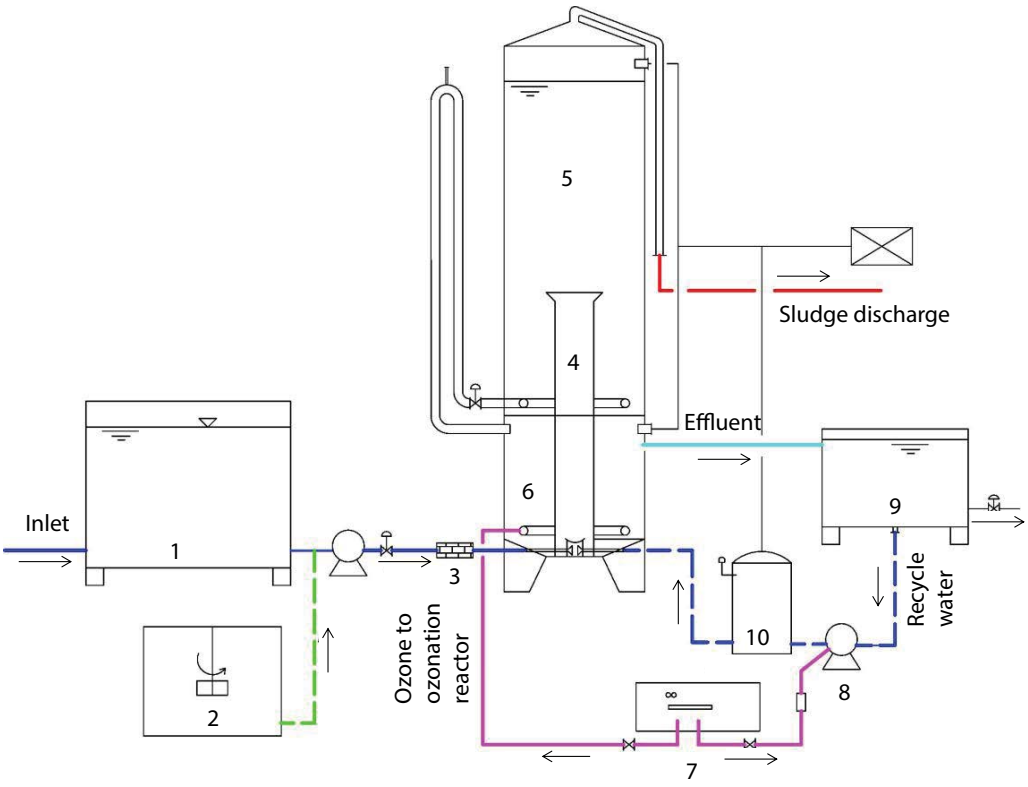

Fig. 1. Experimental setup for DOIF system. (1) Raw water tank; (2) PAC dissolving tank; (3) online mixing; (4) contact zone; (5) separation zone; (6) ozonation reactor; (7) ozone generator; (8) multiphase flow pump; (9) effluent; (10) saturator.

Table 1
Standard operational condition for the DOIF reactor

Parameters	Value
Raw water flow rate, $m^3 h^{-1}$	1.5
Air and gaseous ozone flow rate	0.2 $m^3 h^{-1}$ (at 1 atm)
DOIF separator height[a], m	3.6
Diameter, m	0.8
Surface overflow rate, m h^{-1}	3.0
Online mixing time, s	60
PAC dosage, mg L^{-1}	160
HRT in the DOIF separator, min	50
HRT in the extra ozonation reactor, min	10

[a]Without sludge chamber.

for cleaning. The optical microscope (Nikon SMZ1270i) was positioned at the surface of the system to view the microbubbles and aerated flocs. Qualitative data such as flocs and bubble size distribution can be obtained using image analysis software (NIS-Elements D 3.2). A schematic of the aerated flocs characterization system is shown in Fig. 2.

2.3.2. Water quality analysis

Turbidity was measured by using a Hanna (Shanghai, China) turbidity meter [18] whereas color was measured by the platinum-cobalt method using a UNIC TU-1901 spectrophotometer at 350 nm. TOC and UV_{254} were measured by the

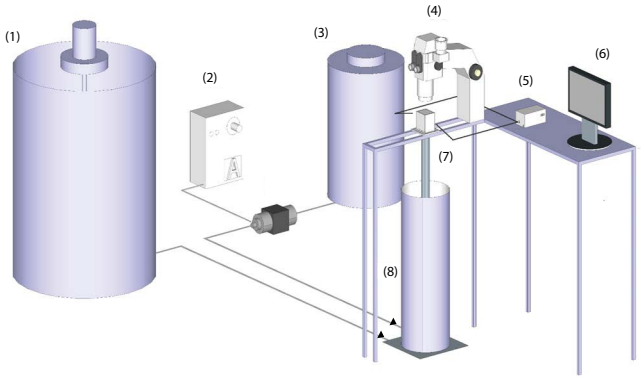

Fig. 2. Schematic of the aerated flocs characterization technique: (1) raw water; (2) ozone generator; (3) recycle water; (4) optical microscope; (5) illumination sources; (6) screen; (7) tube of the aerated flocs characterization technique; (8) flotation cell.

catalytic combustion method using a Shimadzu TOC-VCPH analyzer and a UNIC TU-1901 spectrophotometer at 254 nm (cell length 1 cm), respectively. Total phosphorus was measured using potassium persulfate method. Total coliforms were analyzed by membrane filter technique, and the results were recorded in terms of colony forming unit (cfu) [19].

2.3.3. Fluorescence excitation–emission matrix analysis

Fluorescence measurements were conducted using a spectrofluorometer (FP-6500, JASCO, Japan) equipped with

a 150 W xenon lamp at ambient temperature. A 1 cm quartz cuvette with four optical windows was used for the analyses. Emission scans were performed from 280 to 550 nm at 5 nm steps, with excitation wavelengths from 220 to 480 nm at 2 nm intervals. The slit widths for excitation and emission were 5 nm. The detector was set to high sensitivity and the scanning speed was maintained at 2,000 nm min^{-1} in this study. Under the same conditions, fluorescence spectra for distilled water were subtracted from all the spectra to eliminate water Raman scattering and to reduce other background noise throughout the experimental period.

2.3.4. Molecular weight distribution and para-chlorobenzoic (pCBA) acid analysis

Molecular weight distribution in DOIF system and the concentration of *p*CBA were conducted by high performance liquid chromatography using a LC-2010AHF liquid chromatographic analyzer (Shimadzu, Japan). The characterization of the molecular weight distribution used Zenix SEC-100 gel column and a UV detector at 254 nm. In addition, the mobile phase was 150 mM phosphate buffer solution with a pH of 7.0 ± 0.1 and the velocity was 0.8 mL min^{-1}.

The concentration of hydroxyl radicals in the solution was indirectly monitored by the •OH-probe method. In this study, *p*CBA was selected as •OH-probe not only because it displays slow reactions with ozone ($k_{O3,\ pCBA} \leq 0.15\ M^{-1}\ s^{-1}$) [20] and rapid oxidation kinetics with the •OH radical ($k^{\bullet}_{OH,\ pCBA} = 5 \times 10^{9}\ M^{-1}\ s^{-1}$) [21] but also because it was hardly removed by coagulation process [15]. In addition, sodium thiosulfate (0.025 M) was added to quench •OH in the sampling bottle, preventing its further oxidation. The concentration of *p*CBA was measured using C-18 column and a UV detector at 234 nm. The mobile phase was acetonitrile: H_2O (adjusted to pH 2 with phosphoric acid) = 50:50 and flow rate was kept at 1 mL min^{-1}.

3. Results and discussion

3.1. Effect of saturator pressure and of recycle ratio on the bubbles and aerated flocs size distribution

3.1.1. Effect of saturator pressure and of recycle ratio on the bubbles size distribution

Fig. 3(a) shows the effect of saturator pressure on the bubbles size distribution at 30% recycle ratio. At 0.3 MPa, the bigger bubbles 100–230 μm accounted for 38.63% of the population. Also, at 0.4 MPa, the majority of bubbles (>80%) were smaller than 100 μm while the bigger bubbles 100–140 μm, accounted for just 15.84% of the population. Similarly, at 0.5 MPa, the majority of bubbles (>70%) were smaller than 100 μm while the bigger bubbles 100–220 μm accounted for 24.04% of the population. The average bubble size was 87, 70 and 75 μm at the saturator pressure of 0.3, 0.4 and 0.5 MPa, respectively. The results showed that the smallest bubbles diameter was at 0.4 MPa. In addition, the average size remained steady when the saturation pressure is equal to or higher than 0.4 MPa. According to the previous study by Azevedo et al. [22], this condition guaranteed a small size of microbubbles and high bubble surface area flux, while minimizing energy consumption compared with 0.5 MPa. And this result was similar to that of previous studies [23–25], which implied the limitation of microbubble generation with the control of operational pressure.

Fig. 3(b) shows the effect of recycle ratio on the bubble size distribution at 0.4 MPa. At recycle ratio of 30%, the majority of bubbles (>80%) were smaller than 100 μm while the bigger bubbles 100–140 μm, accounted for just 15.84% of the population. Moreover, the bigger bubbles 100–180 μm accounted for 55.90% and 52.24% of the population at recycle ratio of 30% and 40%, respectively. The average bubble size was 70, 96 and 92 μm at recycle ratio of 30%, 40% and 50%, respectively. The results showed that smallest bubbles diameter was at recycle ratio of 30%. The average microbubbles size at recycle ratio of 40% was larger than that at recycle ratio of 30%, which appeared to be due to the increase of turbulence flow that caused coalescence and growth between bubbles. Moreover, the average size was hardly changed when the recycle ratio was equal or higher than 0.4 MPa. The results showed that the average bubbles size increased with the increase of recycle ratio, likely due to the increase of turbulence flow, which caused coalescence and growth between bubbles. According to the previous study [26], flotation rate was related to bubble size, which should be as small as possible in order to facilitate solid–liquid separation. Therefore, the optimal recycle ratio was 30%, which concurred with recent result [27].

In general, the previous studies [28–31] reported that the size distribution of microbubbles is 30–100 μm. At 0.4 MPa, 30% recycle ratio, the majority of bubbles (>80%) were smaller than 100 μm while the bigger bubbles 100–140 μm, accounted for just 15.84% of the population. As shown in

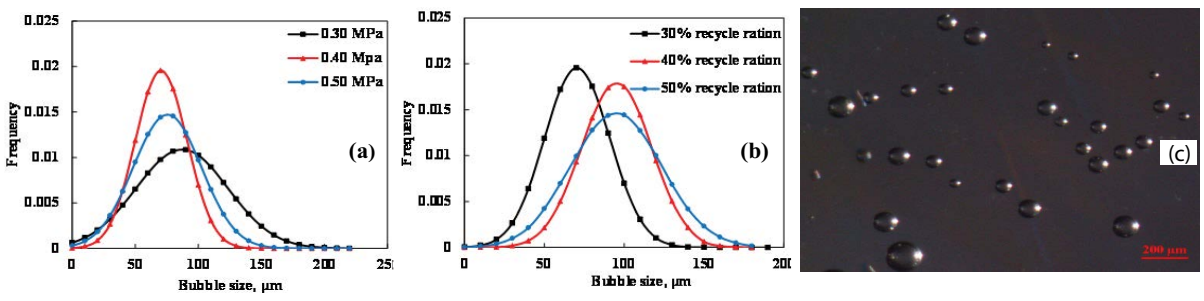

Fig. 3. Bubbles size distribution and their microphotographs. Experimental conditions: (a) at a fixed recycle ratio (30%); (b) at a fixed pressure condition (0.4 MPa); (c) at 0.4 MPa, 30% recycle ratio.

Fig. 3(c), microphotographs of bubbles contained a small amount of large bubbles, which was agreed with the previous studies [32,33] that gave evidence to the presence of these large bubbles. This effect appears to be due to turbulent flow. Overall, the favorable bubbles were generated at 0.4 MPa and 30% recycle ratio.

3.1.2. Effect of saturator pressure and recycle ratio on the aerated floc size distribution

Fig. 4(a) shows the effect of saturator pressure on the aerated flocs size distribution at 30% recycle ratio. The average aerated floc size was 0.50, 0.63 and 0.58 mm at the saturator pressure of 0.3, 0.4 and 0.5 MPa, respectively. The results showed that there were larger aerated flocs at 0.4 MPa compared with other operational conditions. According to the previous study [34], bubbles were entrapped in floc structures, which are favorable to improve rising velocity of the aerated floc, thereby improving solid–liquid separation. Therefore, aerated flocs at 0.4 MPa may contain more number of bubbles, which can be effectively removed.

Fig. 4(b) shows the effect of recycle ratio on the aerated flocs size distribution at 0.4 MPa. The average aerated flocs size generated was 0.63, 0.54 and 0.48 mm at recycle ratio of 30%, 40% and 50%, respectively. These data showed that the number of small flocs increased with the increasing of the recycle rate, which was due to the rupture of large flocs which attributed to the excessive mixture or difficulty growing at rapid flocculation. According to the previous study [35], this fact is especially true when the turbulence causes the aggregates to break due to shear forces generated in the liquid. In addition, the surface area of a floc limits the number of bubbles that can be attached [29,36]. Thus, as the recycle ratio increases, aerated flocs contain less bubbles, which is difficult for solid–liquid separation. The optimal recycle ratio was 30%, which was similar to the recent result [37], and much higher recycle ratios cannot further improve the performance, but just increase the running cost.

Fig. 4(c) shows microphotographs of aerated flocs at 0.4 MPa, 30% recycle ratio, which contained a large number of microbubbles. Like this, aerated flocs were formed at this operation condition, which facilitated solid–liquid separation. To sum up, the favorable aerated flocs were generated at 0.4 MPa and 30% recycle ratio.

3.2. Removal performance by the DOIF at optimal operational condition

3.2.1. Color and turbidity removal performance

DOIF system had good performance for color removal and the extra ozonation can further remove color (Fig. 5(a)). The color in water treatment can be divided into two parts. One is the apparent color, which is caused by suspended solids, and the other is the real color, which is caused by unsaturated carbon bonds and aromatic organic matter. The conventional tertiary wastewater treatment process can work for the removal of apparent color [38], but for real color, the removal performance is often poor [39]. The mechanism of decolorization in the DOIF process is mainly the result of ozonation both in flotation part and extra ozone oxidation, which essentially oxidizes the organic matter to achieve real color removal. Also, the flotation in the DOIF process can remove the apparent color in water. There was relatively good turbidity removal in the flotation part although the turbidity in the raw water was not stable (Fig. 5(b)). However, there was very poor turbidity removal during extra ozonation because ozone oxidation cannot remove suspended particles.

3.2.2. Organic matter removal performance

Figs. 6(a) and (b) show the UV_{254} and TOC removal performance, respectively. The meaning of UV_{254} can reflect the amount of the organic matter that can absorb the UV light at 254 nm such as unsaturated and aromatic organic matter. It was reported that ozone oxidation could achieve a remarkable removal performance of this part of the organic matter. Fig. 6(a) shows that the UV_{254} had stable removal performance throughout the treatment process. As shown in Fig. 6(b), the TOC removal was stable in ozone flotation part and poor in extra ozonation reactor. It could be expected that ozone flotation was mainly responsible for organic matter removal as well as organic matter structure changing. Whereas, extra ozonation can just change the structure because of the very poor TOC removal.

According to Fig. 7, the EEM spectra show that the raw water mainly contained humic-like substances [40]. The fluorescence intensity decreased along the treatment process. It indicated that the aromaticity reduced during the treatment, that is, the organic matter structure was changed. Molecular weight distribution variation in DOIF system is shown in

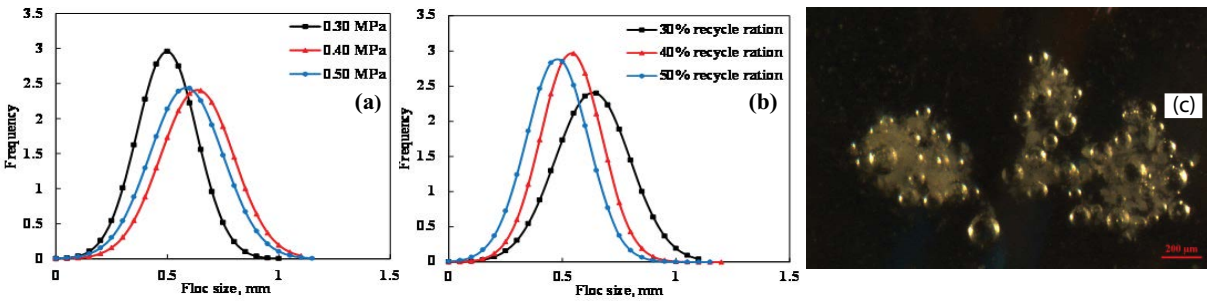

Fig. 4. Aerated floc size distribution and their microphotographs. Experimental conditions: (a) at a fixed recycle ratio (30%); (b) at a fixed pressure condition (0.4 MPa); (c) at 0.4 MPa, 30% recycle ratio.

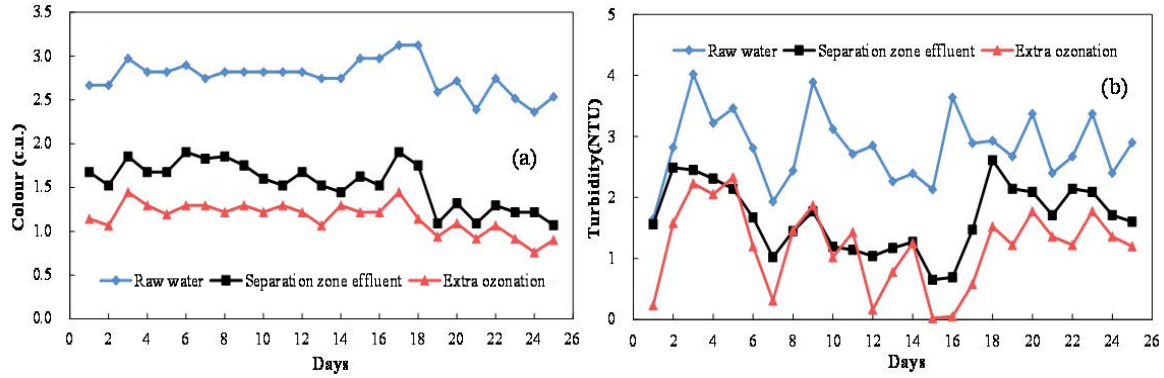

Fig. 5. (a) Color and (b) turbidity removal performance.

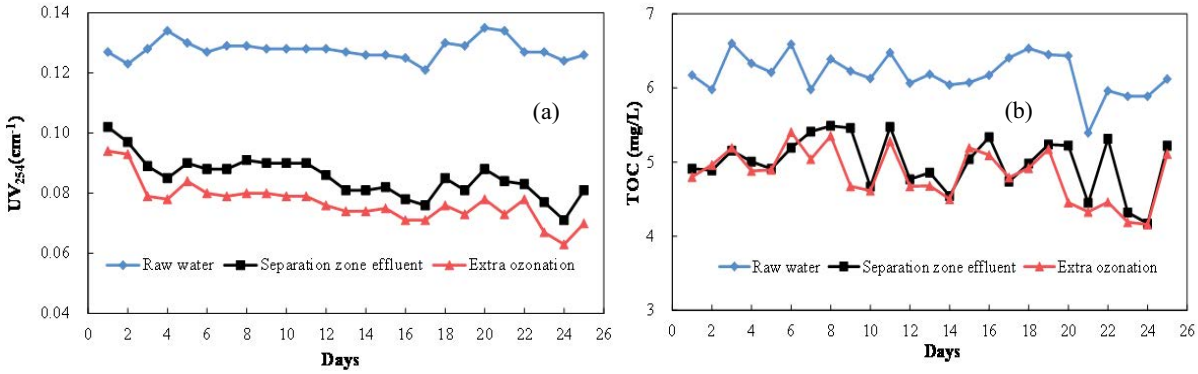

Fig. 6. (a) UV_{254} and (b) TOC removal performance.

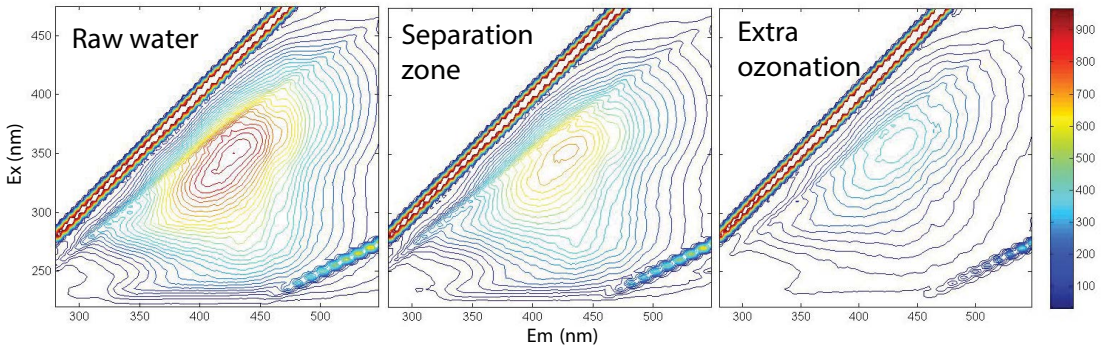

Fig. 7. EEM spectra during treatment process.

Fig. 8. The molecular weight distribution was not changed in ozone flotation section. However, the amount of small molecular weight organic matter increased in extra ozonation section indicating a transformation of high molecular weight organics into small molecular weight organics.

3.2.3. Total phosphorus removal and disinfection performance

Coagulation can remove total phosphorus. Therefore, the DOIF system had high removal efficiency for total phosphorus (Fig. 9(a)), whereas, the extra ozonation section had poor total phosphorus removal. After the tertiary wastewater treatment, the treated water can have several reuse purposes. Whatever the purpose is, the disinfection process is needed to guarantee the safety of the reclaimed water. In the DOIF process, the ozone serves not only as an oxidizer but also as a disinfectant. As shown in Fig. 9(b), the DOIF had very good disinfection performance. Additionally, the extra ozonation reactor can further improve the disinfection effect of the DOIF system.

3.3. Mechanism of DOIF process

Ozone reacts with organic contaminants via the direct oxidation of ozone molecules or the indirect oxidation via hydroxyl radical reaction. In addition, when ozonation and

coagulation occurred simultaneously within a single unit, hydrolyzed products of metal salt coagulants can be used as catalyst to promote the •OH generation, thereby improving the removal efficiency of organic matters [15]. Accordingly, there may be catalytic effects of Al-based coagulant on ozonation in the DOIF process.

In order to investigate the mechanism within the DOIF process, the •OH was indirectly measured via the probe compound *p*CBA. According to the previous study [15], *p*CBA was hardly removed by coagulation. *p*CBA concentration was examined during the DOIF process either with or without PAC. The results were shown in Fig. 10. The DOIF process with PAC promoted the *p*CBA removal, which implied more •OH generation. At the same time, significant decrease in *p*CBA removal was obtained in the presence of tert-butanol, a well-known •OH scavenger, regardless of the presence of PAC. The results above proved the generation of •OH and the involvement of •OH oxidation in the DOIF process. In addition, the previous studies [41,42] confirmed that the surface hydroxyl groups of aluminum oxides as catalysts were favorable for the decomposition of ozone into hydroxyl radical. Ozone can react with hydroxyl groups in the aqueous solution through the basic attractive forces of electrostatic forces or/and hydrogen bonding [43], leading to the decomposition of ozone, then generating •OH through chain reaction. Therefore, in this case, ozone not only reacted with OH^- in aqueous phase to initiate the chain reactions but also with the surface hydroxyl groups of Al-based coagulant to generate •OH.

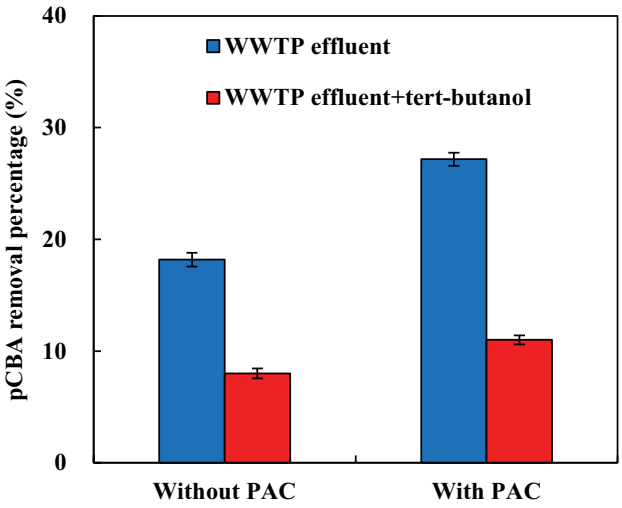

Fig. 10. *p*CBA removal with or without PAC in the DOIF process at 0.4 MPa, 30% recycle ratio.

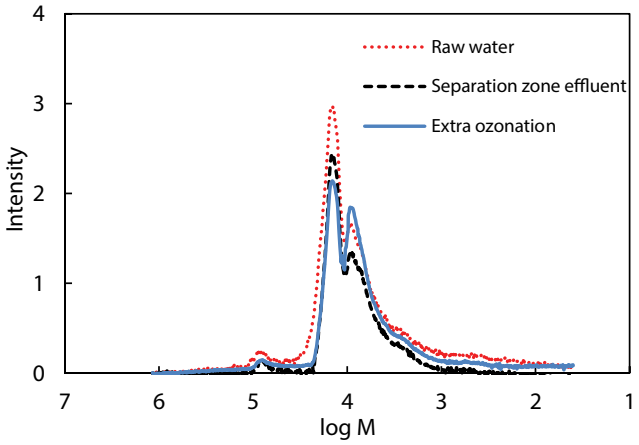

Fig. 8. Molecular weight distribution in DOIF system.

4. Conclusions

A novel DOIF process was developed for application in wastewater reclamation, where ozonation, coagulation and separation occurred simultaneously. Compared with the DOF process, an ozonation zone was added to further oxidize refractory contaminants by residual ozone gas. In this study, a pilot-scale DOIF system fed by secondary effluent from a WWTP in Xi'an, China, was used to evaluate its performance in tertiary wastewater treatment. The results showed that the favorable bubbles and aerated flocs were generated at 0.4 MPa and 30% recycle ratio. At the optimal operational condition, the DOIF process exhibited favorable performance of color, turbidity, UV_{254}, TP removal and disinfection in general. Moreover, DOIF system can use extra ozone which cannot be dissolved to further remove color, UV_{254}, total coliform and therefore reduce the waste of ozone from the ozone generator. The DOIF process generated more •OH in the presence of PAC. At the same time, significant decrease in *p*CBA removal was obtained in the presence of *tert*-butanol, a well-known •OH scavenger, regardless of

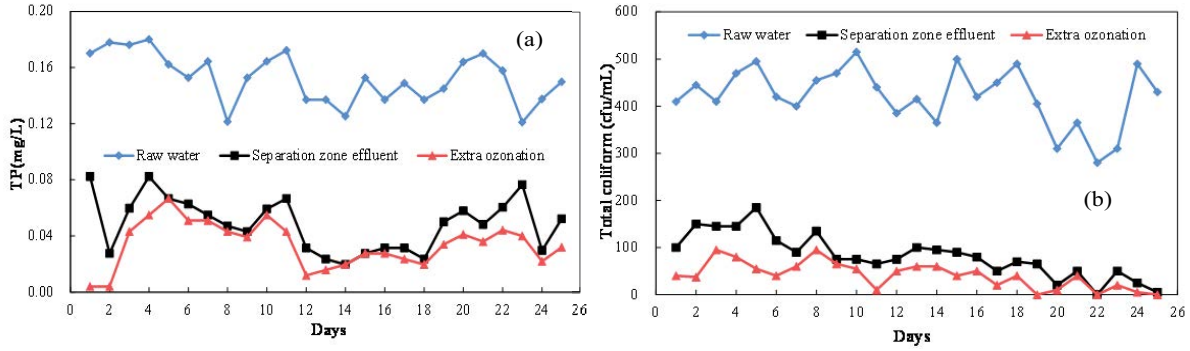

Fig. 9. (a) Total phosphorus removal and (b) disinfection performance.

the presence of PAC. This indicates that the •OH oxidation reaction was involved in the DOIF process and enhanced the removal performance of dissolved organic matter.

Acknowledgments

This study was supported by National Natural Science Foundation of China (Grant No. 51378414, 51708443), National Key Technology Support Program (Grant No. 2014B AC13B06), the Program for Innovative Research Team in Shaanxi (Grant No. 2013KCT-13).

References

[1] J. Jung, H. Park, M. Han, T. Kim, Importance of bubble bed characteristics in Dissolved-air-flotation, Ksce J. Civ. Eng., 2013 (2017) 1–5.
[2] Y. Hwang, M. Maeng, S. Dockko, Development of a hybrid system for advanced wastewater treatment using high-rate settling and a flotation system with ballasted media, Int. Biodeterior. Biodegrad., 113 (2016) 256–261.
[3] J. Haarhoff, Dissolved air flotation: progress and prospects for drinking water treatment, J. Water. Supply Res. Technol., 57 (2008) 555–567.
[4] H.K. Shon, S. Vigneswaran, S.A. Snyder, Effluent organic matter (EfOM) in wastewater: constituents, effects, and treatment, Crit. Rev. Environ. Sci. Technol., 36 (2006) 327–374.
[5] B.H. Lee, W.C. Song, B. Manna, J.K. Ha, Dissolved ozone flotation (DOF) - a promising technology in municipal wastewater treatment, Desal. Wat. Treat., 225 (2008) 260–273.
[6] P.R. Wilinski, J. Naumczyk, Dissolved Ozone Flotation as a Innovative and Prospect Method for Treatment of Micropollutants and Wastewater Treatment Costs Reduction, 12th ed., World Wide Workshop for Young Environmental Scientists, Arcueil, France, 2012, pp. 1–7.
[7] G.A. Oliveira, E. Carissimi, I. Monje-Ramirez, S.B. Velasquez-Orta, R.T. Rodrigues, M.T.O. Ledesma, Comparison between coagulation-flocculation and ozone-flotation for Scenedesmus microalgal biomolecule recovery and nutrient removal from wastewater in a High-Rate Algal Pond, Bioresour. Technol., 259 (2018) 334–342.
[8] J.L. Graham, R. Striebich, C.L. Patterson, K.E. Radha, R.C. Haught, MTBE oxidation byproducts from the treatment of surface waters by ozonation and UV-ozonation, Chemosphere, 54 (2004) 1011–1016.
[9] D.E. John, C.N. Hass, N. Nwachuku, C.P. Gerba, Chlorine and ozone disinfection of *Encephalitozoon intestinalis* spores, Water Res., 39 (2002) 2369–2375.
[10] L. Hu, Z. Xia, Application of ozone micro-nano-bubbles to groundwater remediation, J. Hazard. Mater., 342 (2018) 446–453.
[11] H. Selcuk, Decolorization and detoxification of textile wastewater by ozonation and coagulation processes, Dyes Pigm., 64 (2005) 217–222.
[12] H.Y. Shu, M.C. Chang, Decolorization effects of six azo dyes by O_3, UV/O_3 and UV/H_2O_2 processes, Dyes Pigm., 65 (2005) 25–31.
[13] P. Bose, D.P. Saroj, A. Kumar, Enhancement in mineralization of some natural refractory organic compounds by ozonation-aerobic biodegradation, J. Chem. Technol. Biotechnol., 81 (2005) 115–127.
[14] P.K. Jin, X.C. Wang, G. Hu, A dispersed-ozone flotation (DOF) separator for tertiary wastewater treatment, Water Sci. Technol., 53 (2009) 151–157.
[15] X. Jin, P. Jin, R. Hou, L. Yang, X.C. Wang, Enhanced WWTP effluent organic matter removal in hybrid ozonation-coagulation (HOC) process catalyzed by Al-based coagulant, J. Hazard. Mater., 327 (2017) 216–224.
[16] S. Zhang, S. Gitungo, L. Axe, J.E. Dyksen, R.F. Raczko, A pilot plant study using conventional and advanced water treatment processes: evaluating removal efficiency of indicator compounds representative of pharmaceuticals and personal care products, Water Res., 105 (2016) 85–96.
[17] B.H. Lee, W.C. Song, H.Y. Kim, J.H. Kim, Enhanced separation of water quality parameters in the DAF (Dissolved Air Flotation) system using ozone, Water Sci. Technol., 56 (2007) 149–155.
[18] D. Ma, B. Gao, C. Xia, Y. Wang, Q. Yue, Q. Li, Effects of sludge retention times on reactivity of effluent dissolved organic matter for trihalomethane formation in hybrid powdered activated carbon membrane bioreactors, Bioresour. Technol., 166 (2014) 381–388.
[19] American Public Health Association, Standard Methods for the Examination of Water and Wastewater, 20th ed., Washington, DC, 1998.
[20] C.C.D. Yao, W.R. Haag, Rate constants for direct reactions of ozone with several drinking water contaminants, Water Res., 25 (1991) 761–773.
[21] M.S. Elovitz, U. von Gunten, Hydroxyl Radical/Ozone Ratios During Ozonation Processes. I. The R_{ct} Concept, Ozone Sci. Eng., 21 (1999) 239–260.
[22] A. Azevedo, R. Etchepare, J. Rubio, Raw water clarification by flotation with microbubbles and nanobubbles generated with a multiphase pump, Water Sci. Technol., 75 (2017) 2342–2349.
[23] H.J.B. Couto, M.V. Melo, G. Massarani, Treatment of milk industry effluent by dissolved air flotation, Braz. J. Chem. Eng., 21 (2004) 83–91.
[24] S.J. Kim, J. Choi, Y.T. Jeon, I.C. Lee, C.H. Won, J. Chung, Microbubble-inducing characteristics depending on various nozzle and pressure in dissolved air flotation, Ksec J. Civ. Eng., 19 (2015) 558–563.
[25] S.E. de Rijk, Jaap H.J.M. aivan der Graaf, Jan G. den Blanken, Bubble size in flotation thickening, Water Res., 28 (1994) 465–473.
[26] D. Reay, G.A. Ratcliff, Removal of fine particles from water by dispersed air flotation: Effects of bubble size and particle size on collection efficiency, Can. J. Chem. Eng., 51 (1973) 178–185.
[27] A.I. Zouboulis, A. Avranas, Treatment of oil-in-water emulsions by coagulation and dissolved-air flotation, Colloids Surf. A Physicochem. Eng. Asp., 172 (2000) 153–161.
[28] S. Calgaroto, A. Azevedo, J. Rubio, Separation of amine-insoluble species by flotation with nano and microbubbles, Min. Eng., 89 (2016) 24–29.
[29] J.K. Edzwald, Dissolved air flotation and me, Water Res., 44 (2010) 2077–2106.
[30] D.M. Leppinen, S.B. Dalziel, Bubble size distribution in dissolved air flotation tanks, J. Water Supply Res. Technol., 53 (2004) 531–543.
[31] R.T. Rodrigues, J. Rubio, New basis for measuring the size distribution of bubbles, Min. Eng., 16 (2003) 757–765.
[32] C.O. Rodrigues, Mecanismos De Floculação Com Polímeros Hidrossolúveis, Geração De Flocos Aerados, Floculação Em Núcleos De Bolhas Floculantes E Aplicações Na Separação De Partículas Modelos Por Flotação, PhD Thesis, 2010, p. 242.
[33] C. Oliveira, R.T. Rodrigues, J. Rubio, A new technique for characterizing aerated flocs in a flocculation- microbubble flotation system, Int. J. Miner. Process., 96 (2010) 36–44.
[34] J.K. Edzwald, Principles and applications of dissolved air flotation, Water Sci. Technol., 31 (1995) 1–23.
[35] Y. Hu, G. Qiu, J.D. Miller, Hydrodynamic interactions between particles in aggregation and flotation, Int. J. Miner. Process., 70 (2003) 157–170.
[36] J. Haarhoff, J.K. Edzwald, Modelling of floc-bubble aggregate rise rates in dissolved air flotation, Water Sci. Technol., 43 (2001) 175–184.
[37] R.T. Rodrigues, J. Rubio, Operating parameters affecting the formation of Kaolin aerated flocs in water and wastewater treatment, Clean-Soil Air Water, 42 (2014) 909–916.
[38] M.C. Bongiovani, F.C. Bonggiovani, P.F. Coldebella, K.C. Valverde, L. Nishi, R. Bergamasco, Removal of natural organic matter and trihalomethane minimization by coagulation/flocculation/filtration using a natural tannin, Desal. Wat. Treat., 57 (2016) 5406–5415.
[39] T. Xu, C. Cui, C. Ma, Color composition in a water reservoir and DBPs formation following coagulation and chlorination during its conventional water treatment in northeast of China, Desal. Wat. Treat., 54 (2015) 1375–1384.

[40] J.A. Leenheer, Systematic Approaches to Comprehensive Analyses of Natural Organic Matter, Ann. Environ. Sci., 3 (2009) 1–131.
[41] A. Ikhlaq, D.R. Brown, B. Kasprzyk-Hordern, Mechanisms of catalytic ozonation on alumina and zeolites in water: formation of hydroxyl radicals, Appl. Catal. B Environ., 123–124 (2012) 94–106.
[42] F. Qi, Z. Chen, B. Xu, J. Shen, J. Ma, C. Joll, A. Heitz, Influence of surface texture and acid-base properties on ozone decomposition catalyzed by aluminum (hydroxyl) oxides, Appl. Catal. B Environ., 84 (2008) 684–690.
[43] L. Zhao, Z. Sun, J. Ma, Novel relationship between hydroxyl radical initiation and surface group of ceramic honeycomb supported metals for the catalytic ozonation of nitrobenzene in aqueous solution, Environ. Sci. Technol., 43 (2009) 4157–4163.